Estimate of the Maximum Strength of Metallic Glasses from Finite Deformation Theory

Hao Wang[1,†] and Mo Li[1,2,*]

[1]*School of Materials Science and Engineering, Georgia Institute of Technology, Atlanta, Georgia 30332, USA*
[2]*Department of Mechanical Engineering, Tsinghua University, Beijing 100084, China*

Maximum strength sets the limit of a material's intrinsic resistance to permanent deformation. Its significance, however, lies not in the highest strength value that a solid can possibly achieve, but rather in how this quantity is degraded, from which one could decipher the underlying mechanisms of yielding in a real material. A wide range of maximum strength values have been measured experimentally for metallic glasses. However, the true maximum strength remains unknown to date. Here, using finite deformation theory, we give the first theoretical estimate of the ultimate strength of metallic glasses. Our theoretical results, along with those from experiment and simulation, lead us to several mechanisms of degradation of the theoretical strength that are closely connected to correlated atomic motion with varying characteristic length in real metallic glasses.

Because of the presence of preexisting defects and imperfections in a real crystalline metal, the yield stress is much lower than that in a defect- or imperfection-free sample. The yield stress of the perfect crystal is therefore called the maximum strength, or theoretical strength, as it is often obtained theoretically [1–4]. The significance of the theoretical strength, however, lies not in the maximum strength (MS) value that a solid can possibly achieve but rather in how it is degraded, from which one could decipher the underlying mechanisms for yielding. A classic example is the discovery of crystal dislocations [1–5] which have since become one of the pillars of modern mechanics of crystalline materials.

Different from crystals, metallic glasses (MGs) have no long-range periodic atomic structure and deform plastically at yield point via localized shear [6]. Johnson and Samwer [7] show that experimental yield stress scales universally for a wide range of MGs, about $0.0267G$ at room temperature, where G is the shear modulus from the bulk MG samples. From nanoindentation, Wright, Saha, and Nix [8] obtained the maximum shear stress (MSS) of $0.0808G$ for a $Zr_{40}Ti_{14}Cu_{12}Ni_{10}Be_{24}$ MG. Also using nanoindentation, Bei, Lu, and Gorge determined the MSS of a $Zr_{41}Ti_{14}Cu_{12.5}Ni_{10}Be_{22.5}$ of $0.0829G$ [9]. Recently, Bakai *et al.* [10] reported a MSS about $0.166G$ in a small tip of a $Zr_{41}Ti_{14}Cu_{12.5}Ni_{10}Be_{22}$ needle under electrical ionization potential.

Naturally one would like to ask what the true maximum strength is, or conversely why the strength of real MGs is what it is. Knowing either or both could shed some light on understanding deformation mechanisms in MGs. Presently, we are unable to answer these questions because the theoretical strength for MGs is not available. As a result, the experimentally determined MSs are often compared with those derived for crystals [7–9], which varies from $0.05G$ to $0.2G$, where G is the shear modulus of the crystal, depending on the geometry of the crystal lattice, crystallographic orientation, and the models used for estimation [2,11]. Such comparison may introduce ambiguity in glasses. Therefore, a direct and rigorous theoretical assessment of the true MS for MGs is needed.

Here, we give the first theoretical estimate for the MS for MGs by using a nonlinear elastic theory in a defect-free MG, which is justified by the anticipated large deformation strain corresponding to the maximum stress and the exceedingly large elastic strain limit observed in real MGs, typically 2%–3%. At such large deformation, nonlinear contribution must be considered. Although not being widely recognized, the nonlinear elastic effects are manifested in many properties but determined only in a few cases that are disguised as "anharmonicity" or "structural anisotropy" [12,13]. In the following, we outline the theoretical framework.

Consider a material point in configuration X in a MG, under stress $\sigma_{ij}(X)$ it moves to a new configuration x with a Lagrangian strain η. At a given temperature T, the corresponding Helmholtz free energy $F(x, T) = F(\eta, T)$ at state x can be written as [14]

$$F(\eta, T) = F(0, T) + \tau_{ij}(X)\eta_{ij}V(X) + \frac{1}{2!}C_{ijkl}(X)\eta_{ij}\eta_{kl}V(X) + \frac{1}{3!}c_{ijklmn}(X)\eta_{ij}\eta_{kl}\eta_{mn}V(X)$$

$$+ \frac{1}{4!}\tilde{c}_{ijklmnpq}(X)\eta_{ij}\eta_{kl}\eta_{mn}\eta_{pq}V(X) + \cdots,$$

to the fourth order in η, where $F(0, T) = F(X, T)$,

$$\tau_{ij}(X) = \frac{1}{V(X)} \frac{\partial F}{\partial \eta_{ij}} \bigg|_{X,\eta'},$$

$$C_{ijkl}(X) = \frac{1}{V(X)} \frac{\partial^2 F}{\partial \eta_{ij} \partial \eta_{kl}} \bigg|_{X,\eta'},$$

$$c_{ijklmn}(X) = \frac{1}{V(X)} \frac{\partial^3 F}{\partial \eta_{ij} \partial \eta_{kl} \partial \eta_{mn}} \bigg|_{X,\eta'},$$

and

$$\tilde{c}_{ijklmnpq}(X) = \frac{1}{V(X)} \frac{\partial^4 F}{\partial \eta_{ij} \partial \eta_{kl} \partial \eta_{mn} \partial \eta_{pq}} \bigg|_{X,\eta'}$$

are the corresponding second Piola-Kirchhoff stress, the isothermal second-, third-, and fourth-order elastic constants at state X, respectively. $V(X)$ is the volume of the system. Einstein summation convention is automatically assumed. Similarly, at state x, we can obtain the corresponding stress and the elastic constants,

$$\tau_{ij}(x) = \frac{1}{V(x)} \frac{\partial F}{\partial \xi_{ij}} \bigg|_{x,\xi'},$$

and

$$C_{ijkl}(x) = \frac{1}{V(x)} \frac{\partial^2 F}{\partial \xi_{ij} \partial \xi_{kl}} \bigg|_{x,\xi'},$$

$$c_{ijklmn}(x) = \frac{1}{V(x)} \frac{\partial^3 F}{\partial \xi_{ij} \partial \xi_{kl} \partial \xi_{mn}} \bigg|_{x,\xi'},$$

and

$$\tilde{c}_{ijklmnpq}(x) = \frac{1}{V(x)} \frac{\partial^4 F}{\partial \xi_{ij} \partial \xi_{kl} \partial \xi_{mn} \partial \xi_{pq}} \bigg|_{x,\xi'},$$

where $V(x)$ is the volume of the system and ξ is a Lagrangian strain originated from state x. From these relations, we can connect the stress $\tau(x)$ at any deformed state x to $\tau(X)$ at X via the following relation,

$$\begin{aligned}
\tau_{ij} = (V_0/V) a_{ik} a_{jl} \bigg[& \tau_{kl}(0) + C_{klmn}(0)\eta_{mn} \\
& + \frac{1}{2} c_{klmnpq}(0)\eta_{mn}\eta_{pq} \\
& + \frac{1}{6} \tilde{c}_{klmnpquv}(0)\eta_{mn}\eta_{pq}\eta_{uv} + \cdots \bigg],
\end{aligned} \quad (1)$$

and the elastic constants $C(x)$ to $C(X)$ via

$$\begin{aligned}
C_{ijkl}(x) = (V_0/V) a_{im} a_{jn} a_{kp} a_{lq} \bigg[& C_{mnpq}(0) + c_{mnpquv}(0)\eta_{uv} \\
& + \frac{1}{2} \tilde{c}_{mnpquvxy}(0)\eta_{uv}\eta_{xy} + \cdots \bigg]
\end{aligned} \quad (2)$$

where $a_{ij} = a_{ji} = \partial x_i / \partial X_j$ is the deformation gradient matrix, and $V = V(x)$ and $V_0 = V(X)$.

Equations (1) and (2) furnish the necessary conditions for deriving theoretical strength of MGs if the second-, third-, and fourth-order or higher-order elastic constants are available. Here, we choose the natural state without external applied stress as the reference $X = 0$, i.e. $\tau(0) = 0$. $C(0)$, $c(0)$ and $\tilde{c}(0)$ are the second-, third- and fourth-order elastic constants of the deformation-free sample. When the elastic constants are measured by ultrasound, any pre-existing defect or imperfection will not significantly affect the measurement, if its size is far smaller than the wavelength of sound and remains static [15]. In addition, it is difficult to create new, extended defects by ultrasound in MGs because of the high activation stress needed (as shown below). Thus the glassy material appears "ideal."

The theoretical strength of MGs can be obtained from the theoretical stress-strain relation [Eq. (1)]. But there are two concerns about the effectiveness of the theory. One is the nonaffine deformation often found in amorphous solids. As shown by Weaire et al. [16], however, its effects are already incorporated in our theory through the elastic constants. The second is that the MS obtained from stress-strain relation may not always be the true theoretical strength due to the possible existence of certain elastic instability that is not along the loading path [14,17–20]. This so-called instability bifurcation can be captured from the condition determined by the convexity of the free energy f of the system under strain [20–22], that is,

$$\frac{1}{V(x)} \frac{\partial^2 f}{\partial \eta_{ij} \partial \eta_{kl}} = B_{ijkl}(x) > 0 \quad (3)$$

if the solid is stable; otherwise unstable, where $f = F - W$, F is the Helmholtz free energy and W is the work done to the system by the external stress [20]. $B_{ijkl} = C_{ijkl} + 1/2(\delta_{ik}\tau_{jl} + \delta_{jk}\tau_{il} + \delta_{il}\tau_{jk} + \delta_{jl}\tau_{ik} - 2\delta_{kl}\tau_{ij})$ is the elastic stiffness constant of a MG under external applied stress τ and

$$C_{ijkl} = \frac{1}{V(x)} \frac{\partial^2 F}{\partial \eta_{ij} \partial \eta_{kl}}$$

is the elastic constant in a deformed state x. At the MS, the stability condition is violated such that $|B_{ijkl}| \to 0$. By solving the secular equations, $|B_{ijkl}| = 0$ [20–22], we can obtain the maximum stress τ, as well as the eigenstrain that shows the deformation mode, i.e., shear or cleavage. Note that to solve the stability equation [Eq. (3)], we need to employ Eq. (2). Here we use both the stress-strain relation and the stability condition to obtain the theoretical strength. Since the higher order elastic constants are only available to date for $Zr_{52.5}Ti_5Cu_{17.9}Ni_{14.6}Al_{10}$, $Pd_{40}Cu_{30}Ni_{10}P_{20}$, and $Zr_{41.2}Ti_{13.8}Cu_{12.5}Ni_{10.0}Be_{22.5}$ MGs [23–25], we shall take these results in our theory (see Table I).

For theoretical shear strength, we applied a pure shear deformation to the sample. The corresponding deformation gradient matrix

TABLE I. The experimental second (λ, μ), third (ν_1, ν_2, ν_3), and fourth (γ_1, γ_2, γ_3, γ_4) order Lamé coefficients for three metallic glasses (23–25). Since only three fourth order Lamé coefficients ($\gamma_2 + 0.033\gamma_1$, γ_3, $\gamma_4 + 0.026\gamma_2$) are measured, we varied γ_1 from -1000 to 1000 and did not see significant changes in our results. Here, we take $\gamma_1 = 100$ GPa.

Lamé coefficients, GPa	$Zr_{52.5}Ti_5Cu_{17.9}Ni_{14.6}Al_{10}$	$Pd_{40}Cu_{30}Ni_{10}P_{20}$	$Zr_{41.2}Ti_{13.8}Cu_{12.5}Ni_{10.0}Be_{22.5}$
λ	92.71[a]	136.50[a]	88.34[b]
μ	31.51[a]	34.11[a]	38.17[b]
ν_1	-218.0[a]	-1474.0[a]	-185.1[b]
ν_2	-140.2[a]	-222.0[a,d]	-130.1[b]
ν_3	-35.0[a]	-76.8[a]	-56.1[b]
$\gamma_2 + 0.033\gamma_1$	-338[c]	$\cdots$	$\cdots$
γ_3	398[c]	$\cdots$	$\cdots$
$\gamma_4 + 0.026\gamma_2$	-160[c]	$\cdots$	$\cdots$

[a]Ref. [24].
[b]Ref. [25].
[c]Ref. [23].
[d]A typographic error occurred in Ref. [24]. ν_2 should have a negative sign.

$$a = \begin{pmatrix} 1 + \eta_{11} - \frac{1}{2}(\eta_{11}^2 + \eta_{12}^2) & \eta_{12}(1 - \eta_{11}) & 0 \\ \eta_{12}(1 - \eta_{11}) & 1 + \eta_{22} - \frac{1}{2}(\eta_{22}^2 + \eta_{12}^2) & 0 \\ 0 & 0 & 1 + \eta_{33} \end{pmatrix}$$

and $V_0/V = \det(a)^{-1}$, where η_{12} is the applied shear strain, $\eta_{ii}(i = 1, 2, 3)$ are the normal strains induced by the shear and $\eta_{11} = \eta_{22} \neq \eta_{33}$. From Eq. (1) we get the shear stress τ_{12} to the third order in η_{12}. Figure 1(a) shows the shear stress-strain relations. The values of the MSS are 5.22, 5.77, and 8.73 GPa while the corresponding maximum strain is 0.12, 0.13, and 0.17, respectively. The experimental values of the MSS for the three systems are 0.82 [26], 0.86 [27], and 0.93 [28] GPa, respectively. Figure 1(b) shows that corresponding shear modulus,

$$G = \frac{(C_{11} + C_{12})(C_{33}C_{66} - (C_{36} - \tau_6/2)^2)}{(C_{11} + C_{12})C_{33} - 2C_{13}^2},$$

reaches zero at the maximum stress or strain, and the stability analysis shows that $|\bar{B}|$ approaches zero simultaneously as G at the corresponding maximum shear strain and stress. Here, $|\bar{B}| = [C_{44}C_{55} - (C_{45} + \tau_6)^2](C_{11}^2 - C_{12}^2) \times [C_{33}C_{66} - (C_{36} - \tau_6/2)^2]$, where $\bar{B} = 1/2(B + B^T)$. The Voigt notation is used (11 → 1, 22 → 2, 33 → 3, 23 → 4, 13 → 5, and 12 → 6), such that $C_{1111} \to C_{11}$, $C_{1122} \to C_{12}$, $C_{2313} \to C_{45}$, etc. Similarly, $\tau_{12} = \tau_6$, $\eta_{12} = \eta_6/2$, $\eta_{11} = \eta_1$, etc. Therefore, in pure shear the MS obtained from the stress-strain relation coincides with that from the shear instability analysis.

In Table II we list the theoretical shear stress, strain, and deformation mode for the three MGs. The MS from our theory is around $G/6$ to $G/5$, which coincides with the upper bound of the theoretical stress for close-packed crystalline metals [2,11]. The result confirms the long-held speculation that MG is the strongest among metallic solids. As a comparison, the experimental MSS are about $G/35$ to $G/40$ from bulk samples [7], around $G/10$ in nanoindentation [8,9], and about $G/6$ in a nanowire [10].

Figure 2(a) shows the theoretical tensile and compressive (t/c) stresses. The uniaxial deformation is along the x direction and the deformation gradient matrix

$$a = \begin{pmatrix} 1 \pm \eta_{11} & 0 & 0 \\ 0 & 1 \mp \eta_{22} & 0 \\ 0 & 0 & 1 \mp \eta_{33} \end{pmatrix}.$$

Table II lists the maximum theoretical values at about $E/10$ for tension and $E/7$ for compression of the three MGs.
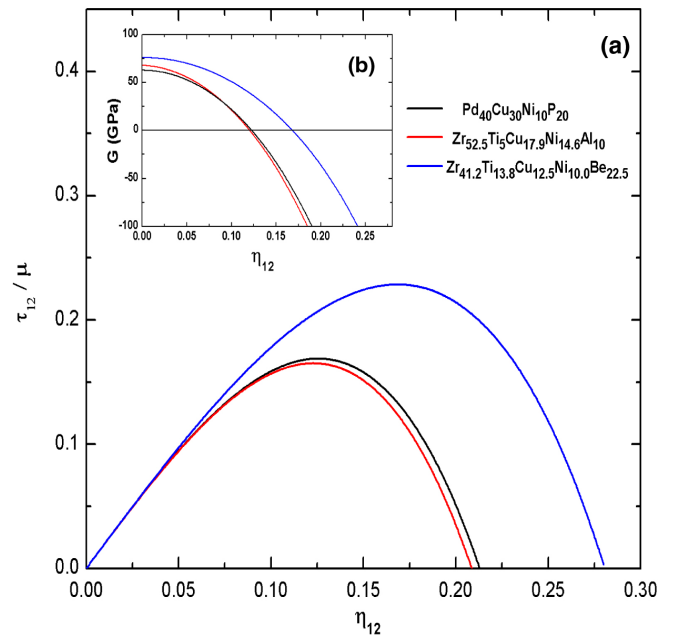
FIG. 1 (color online). (a) The scaled shear stress vs strain. (b) The effective shear modulus vs shear strain.

TABLE II.   The theoretical shear ($\tau^{\max}$), tensile ($\sigma_T^{\max}$), and compressive ($\sigma_C^{\max}$) stress, the corresponding strain, $\gamma^{\max}$, $\eta_T^{\max}$, and $\eta_C^{\max}$, and the deformation mode.

Loading mode	Tension			Compression			Shear		
Deformation mode	$E_{[100]} = 0$			$E_{[100]} = 0$			$G = 0$		
Theoretical stress and strain	$\sigma_T^{\max}$(GPa)	$\sigma_T^{\max}/E$	$\eta_T^{\max}$	$\sigma_C^{\max}$(GPa)	$\sigma_C^{\max}/E$	$\eta_C^{\max}$	$\tau^{\max}$(GPa)	$\tau^{\max}/G$	$\gamma^{\max}$
$Zr_{52.5}Ti_5Cu_{17.9}Ni_{14.6}Al_{10}$	8.65	0.10	0.17	8.51	0.10	0.12	5.22	0.17	0.12
$Zr_{41.2}Ti_{13.8}Cu_{12.5}Ni_{10.0}Be_{22.5}$	7.88	0.08	0.13	16.36	0.16	0.18	8.73	0.23	0.17
$Pd_{40}Cu_{30}Ni_{10}P_{20}$	11.77	0.12	0.08	14.38	0.15	0.11	5.77	0.17	0.13

The experimental compressive yield stress is about $E/50$ (few tensile strength is available) [26–28]. The difference between the maximum t/c stresses indicates strength differential effect or asymmetry observed experimentally. The most intriguing finding though is that there is no shear instability bifurcation observed in uniaxial loading as the maximum t/c stresses at yielding are caused by the instability of Young's stiffness modulus

$$E_{100} = \frac{\bar{B}_{11}(\bar{B}_{22} + \bar{B}_{23}) - 2\bar{B}_{12}^2}{\bar{B}_{22} + \bar{B}_{23}},$$

which goes to zero at the MS [Fig. 2(b)]. The result indicates that different from crystalline metals [14,17,20,29], yielding in an initially isotropic MG under uniaxial loading should occur via cleavage or necking [2,30]. In other words, in an ideal MG, shear is no longer as easy or energetically favorable as in crystals. However, in real MGs localized shear occurs ubiquitously at much lower yield stress [6,7], which contradicts our finding here. In the following, we shall explain this discrepancy by focusing on possible

mechanisms involving correlated atomic motion with some relevant length scales during deformation.

In the finite deformation theory of an ideal glass, each atom subject to external stress participates in the homogeneous deformation; in other words, the atomic motion is correlated and has the characteristic correlation length λ_C approaching the size of the sample. In real MGs, yielding is thought to be caused by groups of atoms [31–33]. Analysis and simulation estimate that the correlated deformation regions grow into the size of about a few hundred atoms with λ_C of about 5 atomic spacing at yielding [7,31–35], which gives rise to the corresponding stress of about $G/40$ in bulk samples [7,31]. For samples under nanoindentation that have higher yield stress [8–10], λ_C is expected to be larger [36] than in bulk samples. For bulk samples, $\lambda_C/a \sim 5$ and $\sigma/\sigma_{\max} \sim 0.130$ [7,31], where $\sigma_{\max} = G/5$ is our theoretical MS and a is the mean atomic spacing. For nanoindentation, $\sigma/\sigma_{\max} \sim 0.415$ [8,9], and the average value for $\lambda_C/a \sim 14$ [34–36]. Note that these data are the only ones existing to date that we are aware of. The trend in Fig. 3 shows clearly that the theoretical strength changes with the correlation length; in other words, the smaller the characteristic size of the correlated atomic motion, the easier for plastic deformation to occur, and the lower the observed yield stress.

FIG. 2 (color online).   (a) The scaled tensile and compressive stress vs strain. (b) The Young's modulus E_{100} vs uniaxial strain.
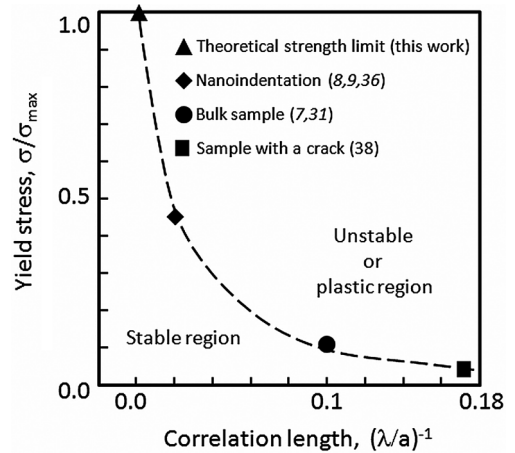
FIG. 3.   The relation between the "achievable maximum strength" and the (inverse) critical length of the correlated atomic motion at the onset of yielding. The dotted line is a guide for the eyes.

The analysis leads us to the following suggestions: (i) if the plastic deformation carriers are deformation regions with correlated atom motion, they should not have fixed structure and size such as dislocations in crystals. They are a function of the achievable yield stress, and vice versa (Fig. 3). Such a unique mechanism is also reflected in the strong sensitivity of MGs' mechanical response to the loading mode [37] that is much less or even absent in crystalline metals. (ii) In real MGs, some locally correlated atomic motion at or near certain structural features can preset λ_C such as casing voids, surface scratches, microcracks, inclusions and second phases, or surface. As suggested by atomistic simulation, the presence of a crack of a nanometer scale can readily initiate shear bands and significantly reduce the strength in a MG [38] by raising local stress [6,39] (Fig. 3). (iii) Conversely, a region already having structural, concentration or chemical inhomogeneity could trigger local shear and thus lead to lower strength. In reality, imperfections with the length scale of a few hundred atomic spacings are not uncommon, even in the nanoscale samples [40–43].

———

*To whom all correspondence should be addressed.
mo.li@mse.gatech.edu

†Present address: Nanosurface Science and Engineering Research Institute, College of Mechatronics and Control Engineering, Sheng Zhen University, Guangdong 518060, China.

[1] M. Polanyi, Z. Phys. **7**, 323 (1921).
[2] J. Frenkel, Z. Phys. **37**, 572 (1926).
[3] E. Orowan, Rep. Prog. Phys. **12**, 185 (1949).
[4] G. I. Taylor, Trans. Faraday Soc. **24**, 121 (1928).
[5] P. B. Hirsch, R. W. Home, and M. J. Whelan, Philos. Mag. **1**, 677 (1956).
[6] C. A. Pampillo, J. Mater. Sci. **10**, 1194 (1975).
[7] W. L. Johnson and K. Samwer, Phys. Rev. Lett. **95**, 195501 (2005).
[8] W. J. Wright, W. R. Saha, and W. D. Nix, Mater. Trans., JIM **42**, 642 (2001).
[9] H. Bei, Z. P. Lu, and E. P. George, Phys. Rev. Lett. **93**, 125504 (2004).
[10] A. S. Bakai, A. P. Shpak, N. Wanderka, S. Kotrechko, T. I. Mazilova, and I. M. Mikhailovskij, J. Non-Cryst. Solids **356**, 1310 (2010).
[11] M. Sob, M. Friak, D. Legut, J. Fiala, and V. Vitek, Mater. Sci. Eng. A **387**, 148 (2004).
[12] Y. Suzuki, J. Haimovich and T. Egami, Phys. Rev. B **35**, 2162 (1987).
[13] E. F. Lambson, W. A. Lambson, J. E. Macdonald, M. R. J. Gibbs, G. A. Saunders, and D. T. Turnbull, Phys. Rev. B **33**, 2380 (1986).
[14] H. Wang and M. Li, Phys. Rev. B **85**, 104103 (2012).
[15] Y. Hiki, Annu. Rev. Mater. Sci. **11**, 51 (1981).
[16] D. Weaire, M. F. Ashby, J. Logan, and M. J. Weins, Acta Metall. **19**, 779 (1971).
[17] H. Wang and M. Li, J. Phys. Condens. Matter **21**, 455401 (2009); **22**, 295405 (2010).
[18] R. Hill and F. Milstein, Phys. Rev. B: Solid State **15**, 3087 (1977).
[19] M. R. Cerny, R. Boyer, M. Sob, and S. Yip, J. Comput.-Aided Mater. Des. **12**, 1611 (2005).
[20] H. Wang and M. Li, J. Phys. Condens. Matter **24**, 245402 (2012).
[21] M. Born, Math. Proc. Cambridge Philos. Soc. **36**, 160 (1940)
[22] R. Furth, Nature (London) **145**, 741 (1940).
[23] N. P. Kobelev, E. L. Kolyvanov, and V. A. Khonik, Phys. Solid State **49**, 1209 (2007).
[24] N. P. Kobelev, E. L. Kolyvanov, and V. A. Khonik, Phys. Solid State **47**, 405 (2005).
[25] R. J. Wang, F. Y. Li, Z. C. Qin, and W. H. Wang, Chin. Phys. Lett. **18**, 414 (2001).
[26] Y. Zhang, D. Q. Zhao, R. J. Wang, and W. H. Wang, Acta Mater. **51**, 1971 (2003).
[27] J. Lu, G. Ravichandran, and W. L. Johnson, Acta Mater. **51**, 3429 (2003).
[28] U. Harms, O. Jin, and R. B. Schwarz, J. Non-Cryst. Solids **317**, 200 (2003).
[29] J. P. Hirth and J. Lothe, *Theory of Dislocations* (Krieger Pub. Co., Malabar, Florida, 1992), 2nd ed.
[30] Q. K. Li and M. Li, Intermetallics **14**, 1005 (2006).
[31] A. Argon, Acta Metall. **27**, 47 (1979).
[32] F. Spaepen, Acta Metall. **25**, 407 (1977).
[33] M. L. Falk and J. S. Langer, Phys. Rev. E **57**, 7192 (1998).
[34] S. Kobayashi, K. Maedak, and S. Takeuchi, Acta Metall. **28**, 1641 (1980); S. G. Mayr, Phys. Rev. Lett. **97**, 195501 (2006).
[35] A. Argon and H. Y. Kuo, Mater. Sci. Eng. **39**, 101 (1979).
[36] D. Pan, A. Inoue, T. Sakura, and M. W. Chen, Proc. Natl. Acad. Sci. U.S.A. **105**, 14 709 (2008).
[37] M. Zhao and M. Li, Metals (Basel, Switz.) **2**, 488 (2012).
[38] Q. K. Li and M. Li, Appl. Phys. Lett. **87**, 031911 (2005); **91**, 231905 (2007).
[39] T. L. Anderson, *Fracture Mechanics: Fundamentals and Applications* (Taylor and Francis, Boca Raton, FL 2005), 2nd ed.
[40] H. Guo, P. F. Yan, Y. B. Wang, J. Tan, Z. F. Zhang, M. L. Sui, and E. Ma, Nat. Mater. **6**, 735 (2007).
[41] D. C. Jang and J. R. Greer, Nat. Mater. **9**, 215 (2007).
[42] L. Tian, Y. Q. Cheng, Z. W. Shan, J. Li, C.-C. Wang, X.-D. Han, J. Sun, and E. Ma, Nat. Commun. **3**, 609 (2012).
[43] T. Ohkubo and Y. Hirotsu, Phys. Rev. B **67**, 094201 (2003).